Nanoscale Advances

PAPER

View Article Online
View Journal | View Issue

Cite this: *Nanoscale Adv.*, 2023, **5**, 5390

Thymoquinone-loaded lipid nanocapsules with promising anticancer activity for colorectal cancer†

Mouna Selmi,[a] Abir Salek,[a] Mahassen Barboura,[a] Leila Njim,[b] Amine Trabelsi,[ac] Aida Lahmar,[a] Nolwenn Lautram,[d] Emilie Roger,[d] Tarek Baati *[e] and Leila chekir Ghedira[a]

Received 23rd June 2023
Accepted 31st July 2023

DOI: 10.1039/d3na00445g

rsc.li/nanoscale-advances

Colorectal cancer (CRC) is the third most common worldwide. Depending on its stage, chemotherapy is usually given after surgery when CRC has already metastasized to other organs like the liver or lungs. Unfortunately, the current antineoplastics used for CRC therapies involve toxicity and side effects due to their lack of site-specificity. To overcome the drawbacks of heavy chemotherapy, this study proposes to assess the efficacy of thymoquinone (TQ), a bioactive constituent of black seeds (*Nigella sativa*), as an antiproliferative and pro-apoptotic agent on an experimental CRC model in mice. TQ was encapsulated in lipid nanocapsules (LNCs), used as nanocarriers, in order to increase its specificity and cell absorption. TQ-loaded LNCs (TQ-LNCs) have a diameter of 58.3 ± 3.7 nm and 87.7 ± 4.5% TQ encapsulation efficiency. In turn, *in vivo* studies showed that the intratumoral administration of TQ-LNCs decreased the tumor size in colorectal cancer bearing mice compared to the control group. TQ-LNCs were more effective than free TQ for inducing tumor cell death. These results highlight the potential of TQ entrapped in LNCs as an anticancer agent for CRC treatment.

1. Introduction

Colorectal cancer (CRC) is the third most common cancer after breast and lung cancer leading to mortality with around 1.93 million cases in 2020.[1] To fight this cancer, chemotherapy drugs, such as 5-fluorouracil, cisplatin, and oxaliplatin, are used in order to destroy fast-growing cancer cells and prevent them from multiplying by interfering with their cell division mechanisms.[2] Despite their anti-cancer efficacy, chemotherapy causes long-term side effects, such as hair loss, nausea, and vomiting,[3] due to their lack of specificity to the site of drug action. Indeed, these medicines kill cancer cells as well as regular cells and consequently cause health complications, which are often very severe for the patient. Hence, there is an ongoing need for new anti-cancer agents exhibiting better toleration, specificity and efficiency in order to overcome the drawbacks of classical chemotherapy. Natural products can be a perfect alternative for the substitution of chemotherapy agents since they exhibit an acceptable therapeutic approach owing to their accessibility, applicability, and reduced cytotoxicity. Several anti-tumor agents have been found in plants, such as thymoquinone (TQ), which is a potent orally active phytochemical obtained from *Nigella sativa* plant. Thymoquinone is commonly used in traditional medicine for its biological activities, such as anti-oxidant, anti-inflammatory, anti-diabetic, gastric ulcer, and cardio protective activities.[4,5] Besides these activities, TQ has been reported to have a potentiel anticancer effect when tested on a range of cancer cell lines, including breast and ovarian adenocarcinoma, lung carcinoma, human pancreatic adenocarcinoma, and CRC.[6–13] Despite its great potency in killing cancer cells, TQ application has often raised several concerns related to its relatively low solubility in water and its rapid elimination after serum opsonin binding, leading to a considerable decease of its bioavailability and pharmacological activity.[14–16] To deal successfully with these drawbacks, numerous studies have tried to encapsulate TQ into organic nanocarriers, used as delivery systems, like lipid-coated mesoporous silica nanoparticles,[17] chitosan-solid lipid nanoparticles,[18] and lipid nanocapsules.[19] Indeed, owing to their high surface and volume ratio, nanocarriers are able to modify the basic properties and to enhance both drug solubility and stability[20,21] and improve drug pharmacokinetics and biodistribution. In addition, nanocarriers significantly decrease drug toxicity through a controlled release mechanism.[20–24] The lipid

[a]*Laboratoire des Substances Naturelles Bioactives et Biotechnologie UR17ES49, Faculté de Médecine Dentaire, Université de Monastir, Tunisia*
[b]*Service d'Anatomie Pathologique, CHU de Monastir, Université de Monastir, Tunisia*
[c]*Laboratoire de Pharmacognosie, Faculté de Pharmacie, Université de Monastir, Tunisia*
[d]*Université d'Angers, INSERM, CNRS, MINT, SFR-ICAT, F-49000 Angers, France*
[e]*Laboratoire des Substances Naturelles, Institut National de Recherche et d'Analyse Physico-chimique, Biotechpôle Sidi Thabet, 2020 Tunisia. E-mail: tarek.baati@gmail.com; Fax: +216 71 537 688; Tel: +216 71 537 666*

† Electronic supplementary information (ESI) available. See DOI: https://doi.org/10.1039/d3na00445g

nanocapsules (LNCs) have gained considerable interest as drug nanocarrier systems (paclitaxel, ferrocifen, and etoposide) as they are highly biodegradable and devoid of toxicity compared to other lipid-based nanocarriers.[25–27] Recently LNCs were successfully synthesized by a high-pressure homogenization method and tested for TQ loading, showing remarkable physiochemical properties, and encapsulation efficiency with stability up to 24 months of storage.[19] Moreover, LNCs were suitable to enhance the pharmacokinetics and biodistribution of TQ after oral and intravenous administration into rats.[19] However, the protocol of LNC synthesis contains oil palm and Tween 80, which could unlikely induce toxicity and health complication. For that we propose in this study to use a safety method to produce ultrapure LNCs without any trace of toxic organic solvent[28] consisting of low-energy emulsification with GRAS (generally recognized as safe) excipients. Following that we determine their loading capacity of thymoquinone and for the first time this new formulation (TQ-LNCs) will be evaluated for intratumoral therapy on a colorectal cancer model subcutaneously developed in mice.

2. Materials and methods

2.1. Materials

Thymoquinone (99%) and DMSO were purchased from Sigma-Aldrich (Saint-Quentin Fallavier, France). Captex® 8000 was provided by Abitec Corp (Saint-Quentin Fallavier, France). Lipoid® S100 and Kolliphor® HS15 were supplied by Lipoid Gmbh (Steinhausen, Switzerland) and BASF (Ludwigshafen, Germany), respectively. Sodium chloride was purchased from Prolabo VWR International (Fontenay-sous-Bois, France). All the other reactants, including HPLC grade acetic acid, acetonitrile, methanol, and water, were purchased from Fisher Scientific (Loughborough, United Kingdom).

2.2. Preparation of thymoquinone-loaded lipid nanocapsules

Thymoquinone-loaded lipid nanocapsules (TQ-LNCs) were prepared according to the original protocol described by Heurtault *et al.*[28] Briefly, 10 mg of TQ were solubilized within Captex® 8000 (13.12% w/w) under magnetic stirring, and then Lipoid® S100 (0.73% w/w) and Kolliphor® HS15 (10.94% w/w) were added. The mixture was then homogenized and supplemented with NaCl (0.8% w/w) and Milli-Q water (19.73% w/w). Next, the preparation was heated to 90 °C, followed by cooling it to 60 °C. Three heating–cooling cycles were applied, followed by a rapid addition at 70 °C of cold water of 2 °C (54.68% w/w). This irreversible thermal shock induces the spontaneous formation of LNCs, which were maintained under moderate stirring for 5 min at room temperature before filtration through a 0.22 μM membrane filter (Merck KGaA, Darmstadt, Germany) in order to remove potential residual components and free TQ. Unloaded LNCs were prepared in a similar manner as describe above without the addition of TQ. All formulations were stored at 4 °C.

2.3 Particle size and zeta potential measurements

The mean particle size, polydispersity index (PDI), and zeta potential measurements of unloaded and TQ-loaded LNCs were determined using a Malvern Zetasizer Nano ZS setup (Malvern Instruments S.A., UK). Before measurement, unloaded LNCs or TQ-LNCs were diluted in deionized water at 1 : 400 (v/v). All measurements were performed at room temperature after equilibration for 2 min. The data were obtained with the average of three measurements.

2.4 Determination of thymoquinone-LNC loading

The encapsulated thymoquinone amount was quantified using ultra performance liquid chromatography (UPLC). The analytical method was developed and validated as described previously with some modifications.[29] Briefly, the analysis was performed using a UPLC-UV Acquity® H-Class Bio separation module (Waters, Saint-Quentin-en-Yvelines, France) equipped with a photodiode array detector (PDA) (Waters) and controlled by Empower software. The analytical column was ACQUITY UPLC BEH C18 1.7 μm, 2.1 × 50 mm I.D. The mobile phase composition consisted of phase A (2% acetic acid in water, pH 2.5) and phase B (methanol), and the separation of TQ was optimized using an isocratic mode (A : B 30 : 70 (v/v)). The flow rate was fixed at 0.2 mL min^{-1} and the run time was 5 min. The retention time of TQ was 1.57 min. The column was operated at 25 °C and TQ was monitored and quantified at 254 nm. The calibration curve was prepared from a stock solution of TQ in methanol at 10 mg mL^{-1}, followed by appropriate dilutions to form concentrations ranging from 5 to 50 μg mL^{-1}. Samples of filtrated TQ-LNCs were diluted by 200 in methanol before the injection of 1 μL. The LNC drug loading capacity (%) was calculated as the amount of total entrapped TQ divided by the total nanoparticle weight. Then the drug loading efficiency (%) was calculated as the ratio of the amount of TQ in the nanoparticles to the total amount of TQ applied in the formulation of the nanoparticles.

2.5 *In vitro* TQ release in an acidic environment from TQ-loaded LNCs

TQ-loaded LNCs were diluted at a final concentration of 10% (v/v) in an acidic solution (pH 4.5) and incubated at 37 °C under continuous shaking at 120 rpm (incubator Multitron Ortibale 50 mm, HT Infors, France). Samples were collected at 0, 0.25, 0.5, 1, 2, 3, 6, 12, and 24 h. Samples were filtered using a 0.2 μm filter to remove free precipitated TQ. All samples were characterized in terms of drug loading using the UPLC method in order to determine the kinetics of TQ release.

2.6 *In vivo* experiments

2.6.1 Cell culture. CT26 murine adenocarcinoma cell lines were provided by the American Type Culture Collection (ATCC, Rockville, MD). Cells were used between passages 2 and 3 and grown in 75 cm^2 flasks at a density of 1 × 10^6 in RPMI-1640 medium (Life Technologies, Gaithersburg, MD) supplemented with 10% fetal bovine serum (FBS, Life

Technologies), 100 U mL^{-1} penicillin and 100 μg mL^{-1} streptomycin (Sigma Aldrich, St. Quentin Fallavier, France). Cells were maintained in culture in a humidified incubator at 37 °C and 5% CO_2. When cells reached 80% of confluence, they were trypsinized and then injected.

2.6.2 Animal model of a subcutaneous colorectal cancer xenograft. Animal care procedures were conducted in conformity with the legislation for the protection of animals used for scientific purposes provided by the relevant Tunisian law and European Union Directive (Tunisian Legislative Decree 2009–2200 and 2010/63/EU) and the International Guiding Principles for the Biomedical Research Involving Animals (Council for the International Organizations of Medical Sciences, CH). Animals were subjected to experimental protocols approved by the Animal Ethics Committee of the Institute of Biotechnology of Monastir (Authorization number: CERSVS/ISBM 009/2022). Twenty-four male BALB/c mice, 5 weeks old, were obtained from the Tunisian Society of Pharmaceutical Industries (SIPHAT, Ben Arous, Tunisia). All animals were maintained in an air-conditioned room (22–25 °C) with a 12 h light/dark cycle. Food and water were available throughout the experimental period. After 7 days of acclimatization, all mice were subcutaneously injected with CT26 murine colorectal cancer cells (2×10^6 cells per mouse, suspended in 100 μL of PBS) in the right flank to form a solid tumor.

2.6.3 Animal treatment. One week after CT26 cell inoculation, when the tumor size grew to an average of 150 mm^3, animals were randomly divided into four groups of six mice ($n = 6$) each depending on the experimental treatment. In the TQ-treated group, TQ was solubilized in 0.1% of DMSO in PBS administrated intratumorally at a dose of 5 mg kg^{-1} body weight of TQ (corresponding to a volume of 80–100 μL). This treatment was repeated every 48 h for 15 days as described by Ma *et al.*, 2017.[30] Similarly, the TQ-LNC group received TQ-LNCs at the equivalent dose of 5 mg kg^{-1} body weight of TQ (corresponding to a volume of 100 μL of LNC). Further, two control groups were treated in the same manner, by intratumoral injection of 100 μL of PBS with 0.1% of DMSO or 100 μL of unloaded LNCs. In all treated groups, the application site was washed twice with 0.9% NaCl and betadine before and after intratumoral injection to avoid local site infection. During the two weeks following the treatment, the body weights and tumor nodule size were measured every 2 days using a caliper. The tumor volumes were calculated using the following formula: $V = L \times W^2 \times 0.523$ (where V is the volume, L is the length, and W is the width).[30]

After two weeks, all animals were anesthetized under isoflurane and sacrificed. Solid tumors from each mouse and organs, including the liver, spleen, heart, lungs, kidneys, and brain, were collected, washed with cooled 0.9% NaCl, weighed and then stored under −20 °C until analysis. The solid tumors were then weighed for tumor inhibitory rate (TIR) determination, which was calculated using the following equation: TIR = ((1 − tumor weight experiment)/tumor weight control) × 100.

2.7 Histology

For histological evaluation, collected organs and solid tumors were immediately fixed in 10% neutral buffered formalin and embedded in a paraffin wax. Sections of 5 μm were cut from each sample and stained with hematoxylin-eosin as reported previously.[31]

2.8 Genotoxicity

The genotoxicity effect of free TQ *versus* TQ-LNCs was assessed by the quantification of DNA damage induced in tumor cells using the comet assay in neutral and alkali conditions as reported previously.[32] Briefly, 10 mg of solid tumor were accurately weighed and then homogenized with 1 mL of PBS. After shaking for 5 min, the homogenate was mixed gently with low melting agarose (1.2%) for cell adhesion and then placed on comet slides for 10 min at 4 °C. Subsequently, cells were incubated in lysis buffer (pH 10) for 1 h at 4 °C in darkness. Next, electrophoresis was performed under neutral condition at 25 V and 300 mA for 15 min and then embedded cells were fixed with ethanol (70%). At the end, comet slides were stained with diluted ethidium bromide (0.02 mg mL^{-1}) and then observed by fluorescence microscopy (Olympus B×51 TRF, USA) using an FITC filter. Finally, the DNA damage percentage was determined according to Eke and Celik 2016, using the following formula: genotoxicity (%) = (total DNA damage of sample − total DNA damage of control/total DNA damage of control) × 100.

2.9 Biochemical parameters

Tumor cytokine levels were measured in a homogenate of 50 mg of tumor mass in 1 mL of PBS using a commercial ELISA kit for GM-CSF (Abcam, ab174448) and TNF-α (Abcam, ab208348).

2.10 Statistical analysis

The data are expressed as mean ± SD. Statistical comparisons among groups were analyzed using one-way and two-way analysis of variance (ANOVA), followed by Tukey's multiple comparison test. Statistical significance was considered for p-value < 0.01.

3. Results

3.1. Nanoparticle characterization

The particles size distribution measured by dynamic light scattering (DLS) shows a mean hydrodynamic size ranging from 56.5 ± 4.7 nm for unloaded LNCs to 58.3 ± 3.7 for TQ-LNCs, indicating no significant difference even when TQ is loaded within nanoparticles (Table 1). Likewise, unloaded LNC and TQ-LNC aqueous suspensions showed a homogeneous monodisperse nanoparticle system according to the polydispersity index, which corresponded to 0.04 ± 0.01 and 0.05 ± 0.02 for unloaded and TQ-loaded nanoparticles, respectively. Moreover, a similar neutral zeta potential (∼3.8 mV) was measured for both formulations, indicating that TQ loading did not influence the surface charge of the nanoparticles. Finally, a nanoparticle

Table 1 Mean particle size, polydispersity index (PDI), and zeta potential values of unloaded LNCs and TQ-LNCs. Drug loading capacity and efficiency of LNCs after filtration ($n = 4$, mean ± SD)

	Size (nm)	PDI	Zeta potential (mV)	Drug loading capacity (%)	Drug loading efficiency (%)
Unloaded LNCs	56.5 ± 4.7	0.04 ± 0.01	3.8 ± 0.5	—	—
TQ-LNCs	58.3 ± 3.7	0.05 ± 0.02	3.8 ± 0.6	7.9 ± 0.8	87.7 ± 4.9

drug loading up to 8.8 ± 0.5 mg mL^{-1} of TQ per LNC suspension was obtained, corresponding to a high drug loading efficiency of 87.7 ± 4.9%.

3.2. Thymoquinone-LNC release

The TQ release profile in acidic medium (pH 4.5) at 37 °C (Fig. 1) showed a burst release of 2.2% of the total encapsulated TQ in LNCs after 0.25 h, followed by an increase to reach 6.4% release after 24 h.

3.3. Antitumor activity of TQ *versus* TQ-LNCs in a subcutaneous tumor xenograft model

The mice treated with free TQ and TQ-LNCs had a significantly high relative weight compared to the control group (Fig. S1†). The anticancer activity of TQ-LNCs was tested on a xenograft model of murine colorectal cancer developed by the injection of CT26 murine colorectal carcinoma cells in the flank of BALB/c mice. Tumor growth was controlled for 15 days following the intratumoral injection of thymoquinone at 5 mg kg^{-1} in solution or encapsulated in LNCs. For the control group (treated with PBS) the average tumor volume increased exponentially from 150 ± 45 mm^3 to 2988.7 ± 99.3 mm^3 at day 15 (Fig. 2B and C).

After the administration of free TQ three times per week, the tumor volume significantly reduced to an average of 1268.3 ± 65.2, corresponding to a substantial tumor growth inhibition by 62.8% ($p < 0.01$) compared to the control group. Moreover, a more drastic tumor regression has occurred after TQ-LNC treatment, resulting in lower tumor volume ranging from 715.1 to 840.3 mm^3, indicating a tumor growth inhibition by 83.4% ($p < 0.01$) compared to the control group. Meanwhile, the tumor growth of unloaded LNC treated mice increased similarly to that of the control group, reaching an average tumor volume

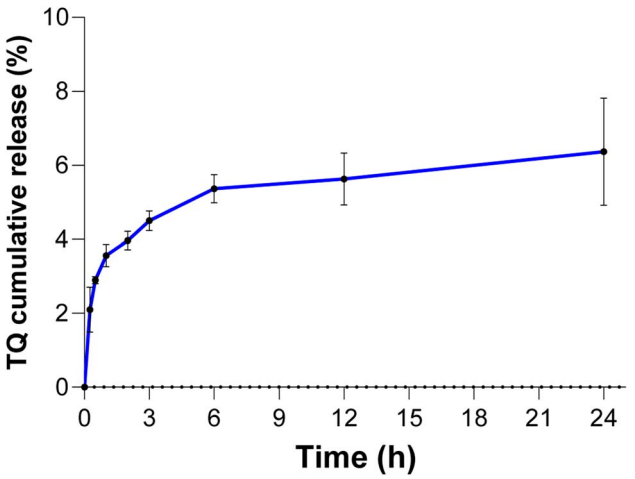

Fig. 1 Cumulative release of TQ in acidic medium (pH 4.5) at 37 °C under continuous stirring. All experiments were carried out in triplicate ($n = 3$).

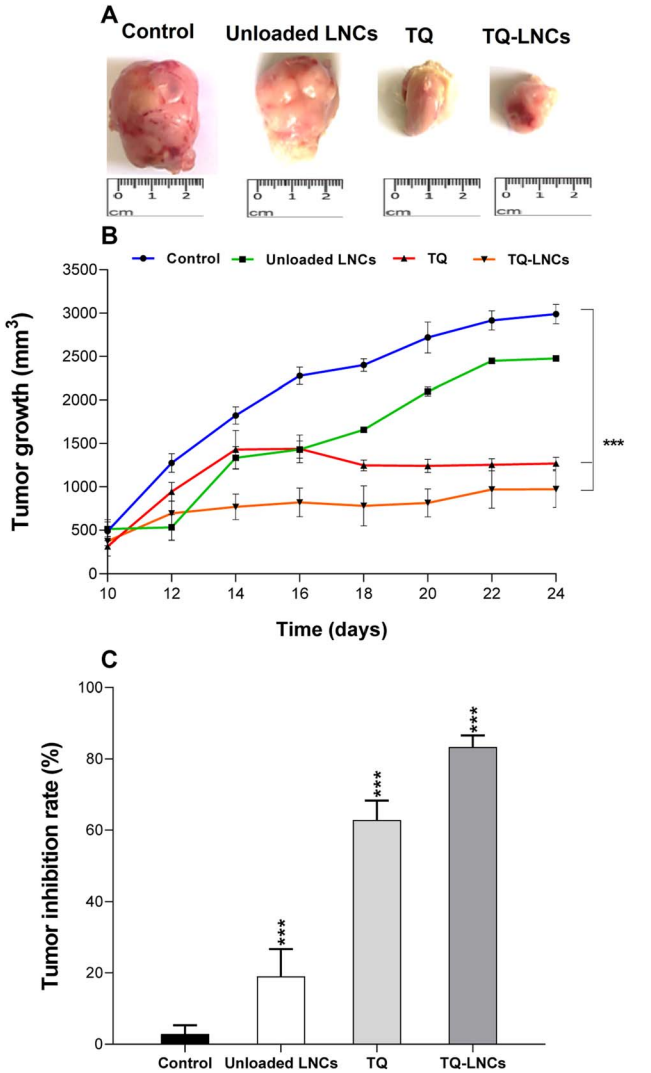

Fig. 2 *In vivo* antitumor effect after intra-tumoral treatment with PBS as control, TQ, and TQ-loaded LNCs at 5 mg kg^{-1} body weight and unloaded LNCs on a subcutaneous colorectal cancer model ($n = 6$ mice/group). (A) Macroscopic effects on mouse tumor at day 15. (B) Progression of mean tumor volume measured using a caliper. (C) Tumor inhibitory rate (***: $P < 0.01$).

of 2600 mm^3, which was not significantly different from that of the control group (3000 mm^3).

3.4. Genotoxicity effect of TQ *versus* TQ-LNCs

DNA damage measurement was conducted using the comet assay to analyze tail parameters in cells isolated from the solid tumors of the control group, unloaded LNCs and mice treated with free TQ and TQ-LNCs at 5 mg kg^{-1}. The treatment with free TQ and TQ-LNCs (Fig. 3A and B) showed a high positive response in the comet assay, indicating the maximum genotoxicity with relative tail moment values of 124.6 ± 1.3 and 138.2 ± 3.6 ($p < 0.01$), respectively. This effect is higher (up to 40-fold) than that of the control group treated with PBS (3.4 ± 1.8) ($p < 0.01$) and unloaded LNC treatment (16.7 ± 1.3). Moreover, the relative tail moment value in the TQ-LNC treated group is almost 1.1-fold ($p < 0.05$) higher than that of the free TQ treated group, evidencing enhanced DNA damage in cancer cells upon LNC mediated drug delivery.

3.5. Effect of free TQ *versus* TQ-LNCs on cytokine levels in tumor tissues

The effect of free TQ and TQ-LNC treatment on the immune system was investigated through the assessment of characteristic cytokine levels, such as GM-CSF and TFN-α, in tumor tissues (Fig. 4A and B). While the unloaded LNCs administered alone did not cause any modification of the GM-CSF and TFN-α levels as compared with the control group, the intratumoral injection of free TQ or TQ-LNCs led to a significant increase in the level of these cytokines, indicating a chronic inflammation. In addition, the levels of cytokines determined in tumors of mice treated with TQ-LNCs are significantly higher than that of mice treated with free TQ ($p < 0.05$).

3.6. Histology

The histopathological sections of the tumor revealed a significant reduction of viable cells in TQ and TQ-LNC groups compared with the unloaded LNCs and control group (Fig. 5). Interestingly, TQ and its nano delivery systems revealed the presence of necrotic areas in tumor sections, evidencing the antitumor potential of TQ and TQ-loaded LNCs. On the other hand, the histopathological examination of liver tissues revealed normal parenchyma regardless of the accumulation of polynuclear neutrophiles as well as in the control group, suggesting a chronic inflammation (Fig. S2†). Furthermore, the histopathological examination of all other organs, including the spleen, kidneys, heart, lungs, and brain, revealed a classical architecture without any apparent change or necrosis in the cellular structures in all treated groups as compared to the control group (Fig. S3–S5†).

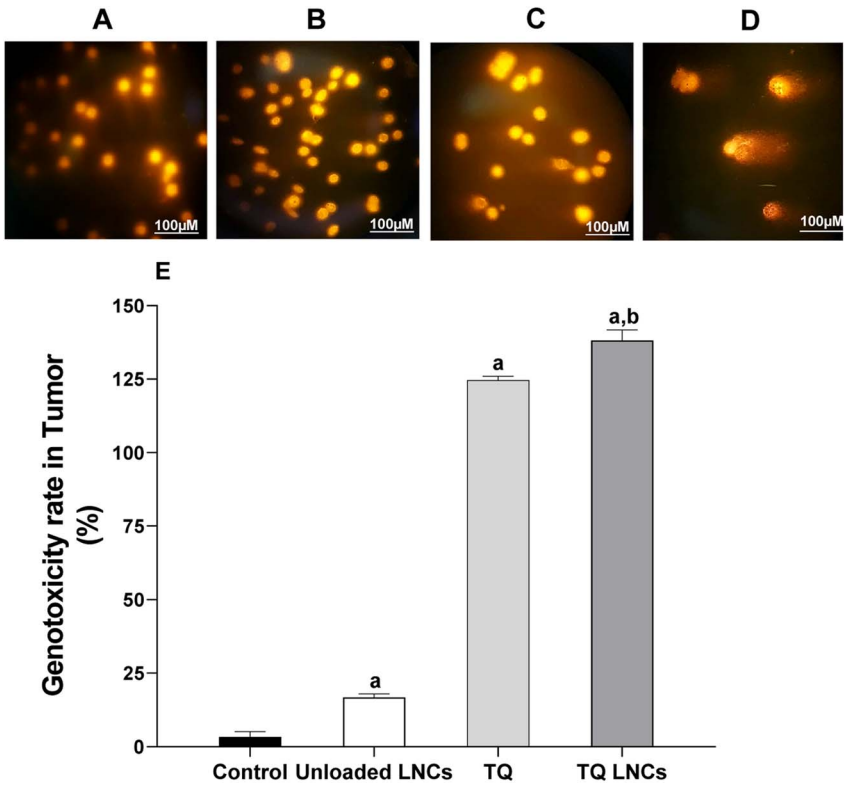

Fig. 3 Comet images of cells isolated from mouse tumors: (A) control and (B–D) treated with unloaded LNCs, free TQ, and TQ-LNCs (at 5 mg kg^{-1} of TQ), respectively. Cells were stained with ethidium bromide (0.02 mg mL^{-1}) and then observed by epifluorescence microscopy using an FITC filter. Magnification = 200×, scale bar = 100 μm. DNA damage in comet cells contains a tail and a head like a comet; apoptotic cells have a large tail and a small head. (E) Effect on total DNA damage assessed through the alkaline comet assay in tumor cells (a: $P < 0.01$ *versus* control group, b: $P < 0.05$ *versus* TQ group).

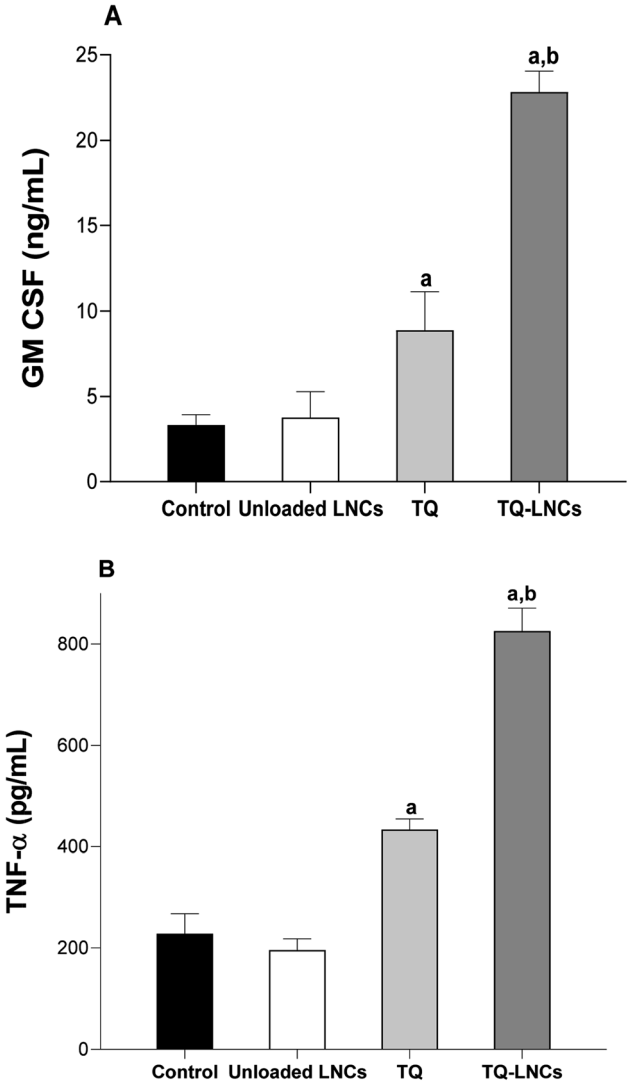

Fig. 4 Effect of TQ and TQ-loaded LNCs on immune system response. Levels of (A) GM-CSF (ng mL^{-1}), and (B) TFN-α (pg mL^{-1}) for the different treated groups (a: $P < 0.05$ *versus* control group, b: $P < 0.05$ *versus* TQ group).

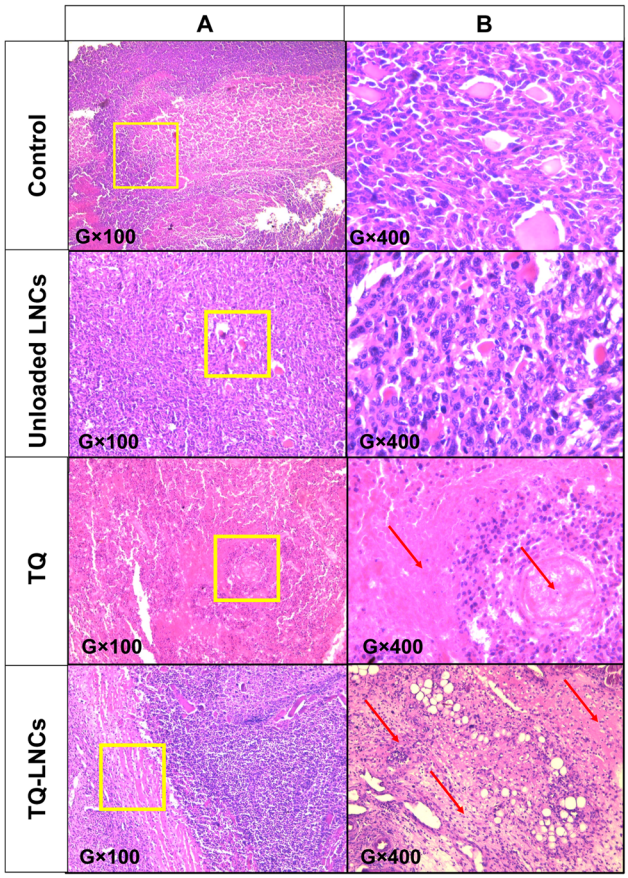

Fig. 5 Histopathology assessments of tumor masses in a subcutaneous colorectal cancer model. Arrows refer to the necrotic areas in tumor tissues after intra-tumoral treatment with PBS (control), unloaded LNCs, free TQ, and TQ-LNCs with a dose of 5 mg kg TQ. (B) is the magnification of the squared area in (A).

4. Discussion

In this study, lipid nanocapsules were synthesized by a phase-inversion process for thymoquinone loading and delivery in order to increase its intratumoral therapy in a colorectal cancer model subcutaneously developed in BALB/C mice. LNCs showed a great drug loading efficiency close to 90% and a drug loading capacity of about 8%. Prior to the *in vivo* experiments, both the unloaded and TQ-loaded LNC suspensions were characterized for their size distribution and surface charge, which play a crucial role in the tumoral cell uptake process. As shown in our experiment, no significant changes were recorded in the hydrodynamic diameter of LNCs due to TQ loading compared to that of the unloaded LNCs. Anyway, TQ-LNCs have been successfully formulated with a mean size less than 100 nm, promising a high tumor cell uptake since the nanoscale size (150–200 nm) decreases the recognition of the phagocytic system and consequently the destruction of nanocarriers.[33,34] Besides the nanoparticle size, the structural abnormalities of the tumor microenvironment contribute to increase the retention of nanocarriers through the enhanced permeability and retention (EPR) phenomenon.[34–38] Indeed, defective angiogenesis develops a high vessel fenestration (150–200 nm) in comparison with the normal vessels, allowing hyperpermeability to the passage of nanoparticles generally with a size lower than 200 nm.[39,40] Moreover, the poor lymphatic drainage of the tumor microenvironment associated with cancer cell proliferation allows not only the accumulation of nanoparticles but also the release of their contents to tumor cells as described for other types of nanoparticles.[40–42]

The acidic tumor microenvironment can modulate the drug release of TQ. *In vitro* release study demonstrated that after incubation under acidic conditions for 24 h, only 6.4% of TQ was released from LNCs, which could be explained by TQ entrapment into the lipid core of the nanocapsule and its protection by the shell composed by Kolliphor®HS15 and Lipoid®S100. Several studies reported the high stability of LNCs loading paclitaxel and Sn[38] under acidic condition incubation

without drug burst effect.[43–46] Moreover, the TQ loading process did not influence the surface charge of TQ-LNCs as compared with the unloaded LNCs. Indeed, the zeta potential of both nanoparticles' suspensions did not shift significantly and took a relatively neutral charge.[47–49] Interestingly, several researches using nanoparticles for drug delivery reported that relatively neutral surface charge enhanced significantly the nanoparticle tumor uptake and reduced their interaction with biological compounds and proteins. Consequently, neutral charge allows nanoparticles to cross easily the cell membranes without the requirement of specific bindings through internalization pathways.[47–49] Thus, these properties of TQ-LNCs enable them to be suitable for application in the treatment of cancer diseases.

Then, the antitumor efficacy of TQ-LNCs has been investigated on mice bearing the colorectal cancer CT26 cell line following intratumoral injection of a relatively high dose of TQ-LNCs (at 5 mg kg^{-1} dose). Fifteen days following the treatment, mice treated with unloaded LNCs showed tumor regression may be attributed to the presence of Kolliphor® HS15 used for synthesis and well known to be toxic at high concentration notably after nanoparticles accumulation in the target tissue with a lethal concentration (LC50) reached 0.427 mg mL^{-1}.[50] Likewise the accumulation of Solutol® HS15 released from LNCs has the ability to inhibit P-gp pump activity and consequently inhibit tumor cell growth.[51,52] On the other hand, mice treated with TQ-LNCs showed a more drastic tumor-growth inhibition of up to 86% without any body-weight loss, evidencing their anticancer efficacy. According to the histopathological assessment, cell necrotic areas decrease significantly in tumor tissues of mice treated with TQ-LNCs compared to those treated with unloaded LNCs and the control group. Meanwhile treatment with free TQ induces less necrosis cells as compared to TQ-LNCs, suggesting lower pharmacological effectiveness probably due to its lipophilicity, which limits its affinity for the tumoral microenvironment and favored its rapid degradation and systemic elimination.[49,50]

The ameliorated anticancer activity observed with TQ upon its entrapment into the LNCs indicates that the lipid nanocapsules improved the drug delivery into the tumor cells, and thus equivalent TQ anticancer activity could be obtained at lower concentrations. This can be explained by the increased number of TQ molecules that are internalized in tumor cells when present in LNCs. Collectively, TQ-LNCs appear to form a better delivery system than free TQ in colorectal cancer treatment without observable toxicity to the other organs, thus improving the efficacy and the therapeutic index of the drug. This proves how the design of TQ-LNCs has gained increasing interest as a means of improving the treatment of neoplastic diseases.[14,15] Altogether, the LNC delivery system enhanced the therapeutic effect of TQ on colorectal cancer through cell apoptosis mechanism and genotoxic effect expressed by cell cycle blocking and DNA damage.[51–53] This was also described for other types of cancers, including breast, ovarian, pancreatic, and lung cancers.[10–12] Similarly, several studies have shown that TQ induces intrinsic apoptotic cell death *via* multiple mechanisms, including the down-regulation of BCL-2 family anti-apoptotic protein expression, activation of the mitochondrial pathway, and caspase expression.[54–59] Commonly, the apoptosis form of death is more favorable than necrosis in eliminating cancer cells as far as it does not induce inflammatory response in the normal cells.[60] Compared to free TQ or TQ-LNC treatment, the immune cytokine levels, such as GM-CSF and TFN-α, determined in tumor tissues increased significantly as compared with those of the unloaded LNCs and control group. These results suggest the induction of a chronic inflammation, which is more expressed in the TQ-LNC group. Thus, LNCs could enhance the resorption of TQ within tumor cells, improving its cytotoxic effect. These results are in accordance with the previous findings, where treatment with TQ increased cytokine levels in breast cancer cells.[54] Regarding the toxicity, all studied parameters, including the healthy behavior of animals and absence of toxicity in the kidneys, spleen, and liver, confirm the biocompatibility of TQ-LNCs. These results clearly confirm the interest in the use of these non-toxic LNCs as a nanocarrier for drug delivery for biomedical applications, notably in cancer therapy.

5. Conclusion

Lipid nanocapsules were synthesized by a phase-inversion process for thymoquinone loading and delivery in order to increase its intratumoral therapy in a colorectal cancer model subcutaneously developed in mice. The main physical parameters (size, shape, and surface charge) that can influence the toxicity of TQ-LNCs were studied and found to be suitable for their bioapplication in cancer therapy. LNCs showed a great thymoquinone loading efficiency close to 90% with slow and sustained release inducing the progressive apoptosis of tumor cells and drastic colorectal tumor regression. This study clearly confirmed the interest in the use of TQ-LNCs in nano-oncology, notably in the treatment of colorectal cancer, and paves the way for the treatment of other types of cancer.

Conflicts of interest

There are no conflicts to declare.

References

1 H. Sung, J. Ferlay, R. L. Siegel, M. Laversanne, I. Soerjomataram, A. Jemal, F. Bray and C. A. Cancer, *J. Clin.*, 2021, **71**, 209–249.
2 B. Viswanath, S. Kim and K. Lee, *Int. J. Nanomed.*, 2016, **11**, 2491.
3 M. S. Aslam, S. Naveed, A. Ahmed, Z. Abbas, I. Gull and M. A. Athar, *J. Cancer Ther.*, 2014, **5**, 817–822.
4 N. E. Abdelmeguid, R. Fakhoury, S. M. Kamal and R. J. Al Wafai, *J. Diabetes*, 2010, **2**, 256–266.
5 S. Padhye, S. Banerjee, A. Ahmad, R. Mohammad and F. H. Sarkar, *Cancer Ther.*, 2008, **6**, 495.
6 S. Darakhshan, A. B. Pour, A. H. Colagar and S. Sisakhtnezhad, *Pharmacol. Res.*, 2015, **95**, 138–158.

7 S. N. Goyal, C. P. Prajapati, P. R. Gore, C. R. Patil, U. B. Mahajan, C. Sharma, S. P. Talla and S. K Ojha, *Front. Pharmacol*, 2017, **8**, 656.
8 M. Imran, R. Rauf, I. A. Khan, M. Shahbaz, T. B. Qaisrani, S. Fatmawati, T. A. Zneid, A. Imran, K. U. Rahman and T. A. Gondal, *Biomed. Pharmacother.*, 2018, **106**, 390–402.
9 S. Idris, B. Refaat, R. Almaimani, H. Ahmed, J. Ahmad and M. Alhadrami, *Life Sci.*, 2022, **296**, 120442.
10 S. H. Jafri, J. Glass, R. Shi, S. Zhang, M. Prince and H. K. Hancock, *J. Exp. Clin. Cancer Res.*, 2010, **29**, 1–11.
11 A. O. Kaseb, K. Chinnakannu, D. Chen, A. Sivanandam, S. Tejwani, M. Menon, Q. P. Dou and G. P. V. Reddy, *Cancer Res.*, 2007, **67**, 7782–7788.
12 A. H. Rahmani, M. A. Alzohairy, M. A. Khan and S. M. Aly, *Evidence-Based Complementary Altern. Med.*, 2014, **10**, 1–13.
13 M. Khan, S. K. Lam, S. Yan, Y. Feng, C. Chen and F. C. F. Ko, *The anti-neoplastic impact of thymoquinone from Nigella sativa on small cell lung cancer: in vitro and in vivo investigations*, Research square, 2023, DOI: **10.21203/rs.3.rs-2434644/v1**.
14 S. A. Pathan, G. K. Jain, S. M. A. Zaidi, S. Akhter, D. Vohora, P. Chander, P. L. Kole, F. J. Ahmada and R. K. Khara, *Biomed. Chromatogr.*, 2011, **25**, 613–620.
15 J. M. M. Salmani, S. Asghar, H. Lv and J. Zhou, *Molecules*, 2014, **19**, 5925–5939.
16 M. A. Khan, M. Tania, S. Fu and J. Fu, *Oncotarget*, 2017, **8**, 51907.
17 I. Rahat, M. Rizwanullah, S. J. Gilani, M. N. Bin-Jummah, S. S. Imam and C. Kala, *J. Drug Delivery Sci. Technol.*, 2021, **64**, 102565.
18 H. M. Fahmy, M. M. Ahmed, A. S. Mohamed, E. S. Eldin and M. T. A. El-Daim, *BMC Pharmacol. Toxicol.*, 2022, **23**, 1–13.
19 F. H. Zakarial Ansar, S. Y. Latifah, W. H. B. Wan Kamal, K. C. Khong, Y. Ng and J. N. Foong, *Int. J. Nanomed.*, 2020, **15**, 7703–7717.
20 E. Cukierman and D. R. Khan, *Biochem. Pharmacol.*, 2010, **80**, 762–770.
21 A. Khan, M. A. Alsahli, M. A. Aljasir, H. Maswadeh, M. A. Mobark and F. Azam, *Pharmaceutics*, 2022, **14**, 153.
22 H. Su, Z. Deng, Y. Liu, Y. Zhao, H. Liu and Z. Zhao, *Mater. Chem. Front.*, 2022, **6**, 1317–1323.
23 A. Aziz, Y. Sefidbakht, S. Rezaei, H. Kouchakzadeh and V. Uskoković, *J. Pharm. Sci.*, 2022, **111**, 1187–1196.
24 L. Woythe, D. Porciani, T. Harzing, S. van Veen, D. H. Burke and L. Albertazzi, *J. Controlled Release*, 2023, **355**, 228–237.
25 S. Peltier, J. M. Oger, F. Lagarce, W. Couet and J. P. Benoît, *Pharm. Res.*, 2006, **23**, 1243–1250.
26 P. Idlas, E. Lepeltier, G. Jaouen and C. Passirani, *Cancers*, 2021, **13**, 2291.
27 J. A. Blanco, V. Sebastián, J. P. Benoit and A. I. T. Suárez, *Eur. J. Pharm. Biopharm.*, 2019, **134**, 126–137.
28 B. Heurtault, P. Saulnier, B. Pech, J. E. Proust and J. P. Benoit, *Pharm. Res.*, 2002, **19**, 875–880.
29 N. Ahmad, R. Ahmad, S. Al Qatifi, M. Alessa, H. Alhajji and M. Saefaroz, *BMC Chem.*, 2020, **14**, 10–15.
30 J. Ma, X. Hu, J. Li, D. Wu, L. Q. Wu and Q. Wang, *Oncotarget.*, 2017, **8**, 85926; Y. S. Ma, J. J. Lin, C. C. Lin, J. C. Lien, S. F. Peng, M. J. Fan, F. T. Hsu and J. G. Chung, *Environ. Toxicol.*, 2018, **33**, 1097–1104.
31 T. Baati, A. A. Kattan, M. A. Esteve, L. Njim, Y. Ryabchikov, F. Chaspoul, M. Hammami, M. Sentis, A. V. Kabashin and D. Braguer, *Sci. Rep.*, 2016, **6**, 1–13.
32 M. B. Imen, F. Chaabane, M. Nadia, K. Soumaya, G. Kamel and C. G. Leila, *Life Sci.*, 2015, **135**, 173–178.
33 J. A. Nagy, S. H. Chang, S. C. Shih, A. M. Dvorak and H. F. Dvorak, *Semin. Thromb. Hemostasis*, 2010, **36**, 321–331.
34 D. Fukumura and R. K. Jain, *J. Cell. Biochem.*, 2007, **101**, 937–949.
35 A. zur Mühlen, C. Schwarz and W. Mehnert, *Eur. J. Pharm. Biopharm.*, 1998, **45**, 149–155.
36 J. S. Choi, C. Cao, M. Naeem, J. Noh, N. Hasan, H. K. Choi and J. W. Yoo, *Colloids Surf., B*, 2014, **122**, 545–551.
37 L. Xu, M. Xu, X. Sun, N. Feliu, L. Feng, W. J. Parak and L. Sijin, *ACS Nano*, 2023, **17**(3), 2039–2052.
38 S. K. Debnath, B. Singh, N. Agrawal and R. Srivastava, EPR-Selective Biodegradable Polymer-Based Nanoparticles for Modulating ROS in the Management of Cervical Cancer, in *Handbook of Oxidative Stress in Cancer: Therapeutic Aspects*, Springer, 2022, 1, p. 28.
39 C. Hoskins, P. K. Thoo-Lin and W. P. Cheng, *Ther. Delivery*, 2012, **3**, 59–79.
40 V. P. Torchilin, *AAPS J.*, 2007, **9**, E128–E147.
41 P. Carmeliet and R. K. Jain, *Nature*, 2000, **407**, 249–257.
42 J. Z. Du, T. M. Sun, W. J. Song, J. Wu and J. Wang, *Angew. Chem.*, 2010, **122**, 3703–3708.
43 J. Liu, Y. Huang, A. Kumar, A. Tan, S. Jin, A. Mozhi and X. J. Liang, *Biotechnol. Adv.*, 2014, **32**, 693–710.
44 E. Roger, F. Lagarce, E. Garcion and J. P. Benoit, *J. Controlled Release*, 2009, **140**, 174–181.
45 E. Roger, F. Lagarce and J. P. Benoit, *Eur. J. Pharm. Biopharm.*, 2011, **79**, 181–188.
46 A. Villanueva, M. Canete, A. G. Roca, M. Calero, S. V. Verdaguer, C. J. Serna, M. D. P. Morales and R. Miranda, *Nanotechnology*, 2009, **20**, 115103.
47 A. M. Bannunah, D. Vllasaliu, J. Lord and S. Stolnik, *Mol. Pharm.*, 2014, **11**, 4363–4373.
48 C. He, Y. Hu, L. Yin, C. Tang and C. Yin, *Biomaterials*, 2010, **31**, 3657–3666.
49 B. M. Razavi and H. Hosseinzadeh, *J. Endocrinol. Invest.*, 2014, **37**, 1031–1040.
50 K. M. Alkharfy, F. A. Ali, M. A. Alkharfy, B. L. Jan, M. Raish, S. Alqahtani and A. Ahmad, *Xenobiotica*, 2020, **50**, 858–862.
51 S. Al Bitar, F. Ballout, A. Monzer, M. Kanso, N. Saheb, D. Mukherji, W. Faraj, A. Tawil, S. Doughan, M. Hussein, W. Abou Kheir and H. G. Muhtasib, *Cancers*, 2022, **2022**(14), 1363.
52 F. Ballout, A. Monzer, M. Fatfat, H. E. Ouweini, M. A. Jaffa, R. A. Samad, N. Darwiche, W. A. Kheir and H. G. Muhtasib, *Oncotarget*, 2020, **11**, 2959.
53 H. G. Muhtasib, M. Diab assaf, C. Boltze, J. Alhmaira I, R. Hartig, A. Roessner and R. Schneider Stock, *Int. J. Oncol.*, 2004, **25**, 857–866.
54 O. H. Alobaedi, W. H. Talib and I. A. Basheti, *Asian Pac. J. Trop. Med.*, 2017, **10**, 400–408.

55 W. Asfour, S. Almadi and L. Haffar, *Sci Reas*, 2013, **4**, 11.
56 C. C. Woo, A. Hsu, A. P. Kumar, G. Sethi and K. H. B. Tan, *PLoS One*, 2013, **8**, e75356.
57 F. Alhmied, A. Alammar, B. Alsultan, M. Alshehri and F. H. Pottoo, *Comb. Chem. High Throughput Screening*, 2021, **24**, 1644–1653.
58 R. Khalife, M. H. Hodroj, R. Fakhoury and S. Rizk, *Planta Med.*, 2016, **82**, 312–321.
59 R. Schneider-Stock, I. H. Fakhoury, A. M. Zaki, C. O. ElBaba and H. U. G. Muhtasib, *Drug Discovery Today*, 2014, **19**, 18–30.
60 G. Kroemer, B. Dallaporta and M. R. Rigon, *Annu. Rev. Physiol.*, 1998, **60**, 619–642.